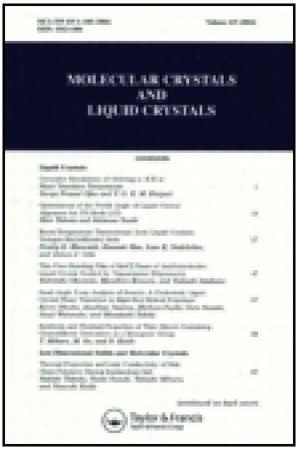

Molecular Crystals and Liquid Crystals Science and Technology. Section A. Molecular Crystals and Liquid Crystals

Publication details, including instructions for authors and subscription information:
http://www.tandfonline.com/loi/gmcl19

Quantifying Azimuthal Anchoring of Nematics using In-Plane Fields and Fully-Leaky Guided Modes

B. T. Hallam [a] & J. R. Sambles [a]

[a] Thin Film Photonics, School of Physics, University of Exeter, Stocker Road, Exeter, EX4 4QL, UK

Version of record first published: 24 Sep 2006

Mol. Cryst. and Liq. Cryst., 2000, Vol. 351, pp. 87-94
Reprints available directly from the publisher
Photocopying permitted by license only

Quantifying Azimuthal Anchoring of Nematics using In-Plane Fields and Fully-Leaky Guided Modes

B. T. HALLAM and J. R. SAMBLES

Thin Film Photonics, School of Physics, University of Exeter, Stocker Road, Exeter, EX4 4QL, UK.

In this work we present a new optical guided mode technique which is used to monitor small perturbations to the director twist profile in a conventional liquid crystal cell. The cell is filled with nematic liquid crystal E7 which is homogeneously aligned using rubbed polyimide. Twist distortions are induced via the application of weak in-plane electric fields. Careful analysis of these distortions allows both the twist elastic constant, k_{22}, and the azimuthal anchoring strength, W_a, of the cell to be determined.

Keywords: Optical waveguides; azimuthal anchoring energy; twist elastic constant

INTRODUCTION

The use of optical guided modes to explore the optical tensor profile of liquid crystals is well established[1,2]. In the present work a new optical guided mode technique, the fully-leaky guided mode technique (FLGM)[3], has been used to study for the first time a conventional (off-the-shelf) cell geometry which comprises standard index glass (n=1.52). This cell is bounded by prisms of an equal refractive index which are optically matched to the cell by a suitably mixed silicone oil index-matching fluid. Hence the cell may be rotated with respect to the prisms. The first prism increases the available in-plane momentum of the incident laser light allowing coupling to a number of leaky modes within the liquid crystal layer. Because both liquid crystal refractive indices are higher than the surrounding glass index, these are not true guided modes and are able to 'leak' into both the incident and transmitted half-spaces. Despite this, each mode has a different optical field profile within the layer and therefore spatially samples the different regions of the cell thickness. Figure 1 shows a typical model reflectivity for HeNe (λ_0=632.8nm) laser light incident on a 1μm thick layer of nematic E7 ($\varepsilon_{\parallel}$=2.282, $\varepsilon_{\perp}$=2.995) bounded by standard index glass. Both the incident and detected polarisations are set to be s-polarised. Each of the broad, angle dependent, reductions in reflectivity shown in figure 1 are due to the light coupling into a leaky guided mode.

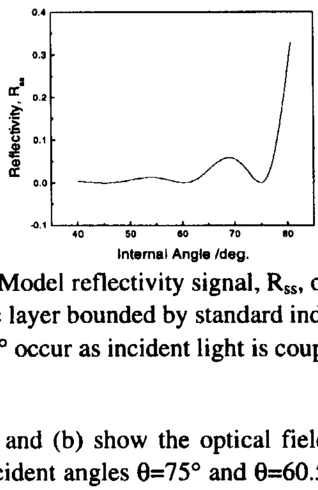

FIGURE 1 Model reflectivity signal, R_{ss}, of light incident on a 1μm nematic layer bounded by standard index glass. Minima at 75° and 60.5° occur as incident light is coupled into leaky modes.

Figures 2(a) and (b) show the optical field profiles for two of these features (at incident angles θ=75° and θ=60.5°). The field profile in figure 2(a) has a maxima in the centre of the cell and is relatively insensitive to the other regions of the liquid crystal. Whereas, the field in figure 2(b) is clearly sampling the upper and lower third of the cell thickness. Hence, by exciting a sufficient number of modes we may be sensitive to the director profile through the entire cell thickness.

Eight different optical data sets may be recorded. These comprise, for reflection (R) and transmission (T): R_{pp}, R_{ps}, R_{sp}, R_{ss}, T_{pp}, T_{ps}, T_{sp} and T_{ss}, where the first subscript denotes the incident polarisation and the second subscript denotes the recorded polarisation.

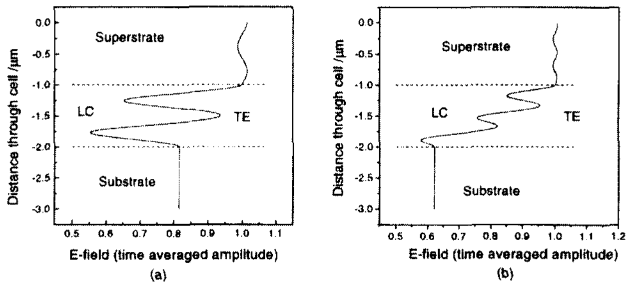

FIGURE 2 Electric-field distributions for s-polarised light incident on 1µm nematic layer bounded by standard index glass. (a) at an incident angle of 75°, (b) at an incident angle of 60.5°.

These data sets can be used to check the resulting model of the director profile since a true director description will give theoretical reflectivities and transmissivities which will fit all eight data sets.

The cell geometry used in this study is shown in figure 3. Homogeneous alignment of the liquid crystal (nematic E7) director is achieved via polyimide layers which are rubbed along the direction of the electrode edges. Gold electrodes (350nm thick) allow an electric field (10kHz a.c.) to be applied within the plane of the substrate. The twist distortions induced by the in-plane field may be compared with continuum theory, allowing both the twist elastic constant, k_{22}, and the azimuthal anchoring energy strength, W_a, to be determined.

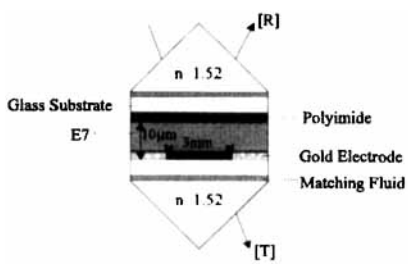

FIGURE 3 A slice through the incident plane of the experimental cell geometry. A silicone oil is used to index-match the cell to the standard index glass prisms.

THEORY

The twist deformation induced in a nematic liquid crystal layer via an in-plane electric field is governed by the Euler-Lagrange equation associated with the change in the free-energy of the nematic subject to the in-plane field:

$$\frac{d^2\phi}{dz^2} = -\frac{\varepsilon_0 \Delta\varepsilon}{k_{22}} \sin\phi\cos\phi \tag{1}$$

Where, $\phi=\phi(z)$ is the twist angle of the nematic, z is the direction through the cell thickness and $\Delta\varepsilon$ is the dielectric anisotropy of the material.

This equation can be solved for the boundary conditions supplied by the torque-balance equations assuming finite surface anchoring (where the anchoring strength on the top surface, W_{a1}, does not have to equal the anchoring strength on the bottom surface, W_{a2}) and a zero-field pre-twist in the cell.

Hence, if $\Delta\varepsilon$ is known together with the magnitude of the applied electric field, the zero-field surface twist angles and the cell thickness; the twist profile of the director through the cell can be generated by choosing values of the constants k_{22}, W_{a1} and W_{a2}. A multilayer optical theory is then used to generate angle-dependent optical data from this profile which serves as model predictions for several different electric field strengths.

The form of the electric field magnitude can be determined by solving Laplace's equation for a scalar field (Φ) between two semi-infinite flat electrodes separated by an in-plane gap g. If there exists a potential difference, V, between the plates, then the associated field lines and equipotentials can be described in an elliptic-cylindrical co-ordinate frame (u, v, z) where:

$$x = \frac{g}{2}\cosh u \cos v \tag{2}$$

$$y = \frac{g}{2}\sinh u \sin v \tag{3}$$

$$z = z \tag{4}$$

Assuming the right-hand electrode corresponds to v=0 with Φ=0, and the left-hand electrode corresponds to v=π with Φ=V, hence:

$$\Phi = \frac{V}{\pi}.v \tag{5}$$

From equations (2) and (3) we find:

$$\frac{x^2}{\cos^2 v} - \frac{y^2}{\sin^2 v} = \left(\frac{g}{2}\right)^2 \tag{6}$$

which is the description of a hyperbola. In the plane of the electrodes (y=0) we find:

$$v = \cos^{-1}\left(\frac{x}{a}\right) \tag{7}$$

Substituting (7) into (5) and solving (8):

$$\underline{E} = -\underline{\nabla}\Phi \tag{8}$$

we find that in the electrode centre (x=0):

$$E = \frac{2V}{\pi g} \tag{9}$$

EXPERIMENTAL

The cell geometry is shown in figure 3. A cell thickness of approximately 10μm was obtained using beaded glue. A 10kHz a.c. signal was applied across the 3mm electrode gap to provide the electric field. The cell was placed on the centre of rotation of a rotating table in a temperature stabilised environment and illuminated with HeNe (λ_0=632.8nm) laser light which had a beam spot area of approximately 0.5mm^2 (significantly smaller than the 3mm electrode gap). The polarisation of the incident, and subsequently the reflected and transmitted signals, were controlled with polarisers. Angle-dependent optical data was collected for a variety of different electric field strengths.

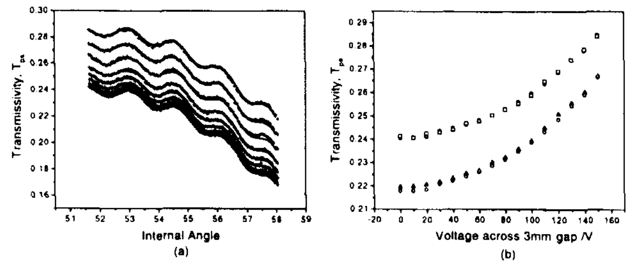

FIGURE 4 The effect of in-plane electric fields on the transmission signal T_{ps} at an azimuthal angle of 53°. (a) Experimental data (+) and theoretical predictions (-) to several different field strengths, (b) the effect on T_{ps} as a function of field strength for fixed angles of incidence, θ=51.75° (squares), θ=55.00° (Δ), model predictions (o).

RESULTS AND DISCUSSION

Figures 4(a) and (b) show the effect on the transmission polarisation conversion signal, T_{ps}, of the applied electric field. The experimental data points are shown as crosses and the theoretical predictions as a solid line. In the analysis of the data the value for the dielectric anisotropy was taken from the literature ($\Delta\varepsilon=14.1$)[4]; yielding the following parameters at room temperature (23.5°C) for E7 on rubbed polyimide: $k_{22}=(6.50\pm0.05)\times10^{-12}$N and $W_{a1}=W_{a2}=(2.9\pm0.2)\times10^{-5}$Jm^{-2}. These results are in good agreement with previously published work[5-7].

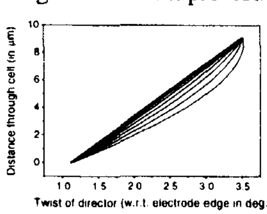

FIGURE 5 The twist profile of the liquid crystal for increasing field strengths.

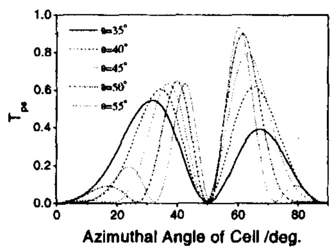

FIGURE 6 Modelling the transmission signal, T_{ps}, as a function of the azimuthal angle of the cell for fixed angles of incidence.

The twist profiles used to generate these model predictions are shown in figure 5. The cell azimuthal angle was carefully chosen to be sensitive to twist distortions. Modelling this transmission signal, T_{ps}, at fixed angles of incidence as the cell is rotated about a plane normal to the incidence plane (figure 6), shows the expected change in optical signal for a given (induced) twist of the cell. The data shown in figure 4 was collected with the cell at an azimuthal angle of 53° where there is a steep gradient. This represents a position which experiences a large change in optical signal for a unit change in the cell twist. Experimental data collected at an azimuthal angle of 50° would not show the same sensitivity to field-induced twist deformations (figure 7) despite the distorted twist profiles being identical.

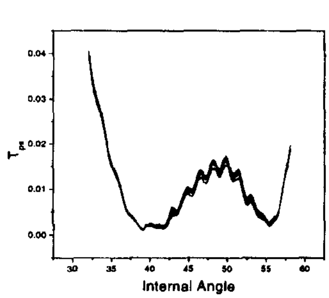

FIGURE 7 The effect of electric field on the transmission signal T_{ps} at a cell azimuthal angle of 50°.

SUMMARY

A new optical guided mode technique has been introduced. This technique has allowed the examination of a conventional cell and has proven to be ideal for the study of very small perturbations to the director profile. The twist elastic constant and the azimuthal anchoring strength of the cell have also been obtained. Continuing this study as a function of temperature will yield information about the surface order parameter.

Acknowledgements
The authors gratefully acknowledge the support of EPSRC and DERA (Malvern).

References

[1] F. Yang and J. R. Sambles, *J. Opt. Soc. Amer.,* **B10,** 858, (1993).
[2] K. R. Welford and J. R. Sambles, *Appl. Phys. Lett.,* **50,** 871, (1987).
[3] F. Yang and J. R. Sambles, *J. Opt. Soc. Amer.,* **B16,** 488, (1999).
[4] T. W. Priest, K. R. Welford and J. R. Sambles, *Liquid Cryst.,* **4,** 103, (1989).
[5] M. S. Bancroft, PhD Thesis, University of Manchester, (1991).
[6] Y. Iimura, N. Kobayashi and S. Kobayashi, *Jpn. J. Appl. Phys.,* **33,** L434, (1994).
[7] J. Min, H. Ximin, W. Zongkai, M. Kai, S. Ruipeng and Z. Xinyi, *Liquid Cryst.,* **18,** 419, (1995).